Performance Analysis of FS-FBMC/OQAM Systems using Companding and Channel Coding Techniques in Rayleigh Fading Channels

Anam Mobin
Department of Electronics and Communication Engineering
Jamia Millia Islamia, New Delhi, India

Anwar Ahmad
Department of Electronics and Communication Engineering
Jamia Millia Islamia, New Delhi, India

ABSTRACT
Filter Bank Multicarrier (FBMC) with offset QAM (OQAM) is a potential waveform contender for 5G and future wireless systems. It can be implemented using either polyphase network (PPN)-FFT or Frequency Spread (FS)-FBMC implementation. It suffers from high peak-to-average-power ratio (PAPR) problem because of its multicarrier nature. In this paper some non-linear companding PAPR reduction techniques such as μ-law, A-law, rooting, tangent rooting, and logarithmic rooting were investigated in terms of their bit-error-rate (BER) performance for FS-FBMC/OQAM systems in Rayleigh flat fading channels. Also, some channel coding techniques such as turbo codes and low-density parity check (LDPC) codes were also investigated in terms of their effect on PAPR value and BER reduction performance for FS-FBMC/OQAM systems in Rayleigh flat fading channels. It was observed that the rooting companding provided better BER performance in comparison to other companding schemes. It was observed that LDPC coded FS-FBMC/OQAM system provided slightly better BER performance in comparison to turbo coded FS-FBMC/OQAM system. It was also observed that LDPC coded FS-FBMC/OQAM system provided lower PAPR in comparison to turbo coded FS-FBMC/OQAM system and is suitable for applications requiring lower computational complexity and delay. It was also observed that the FS-FBMC/OQAM system outperforms the Orthogonal Frequency Division Multiplexing (OFDM)system in terms of BER performance in Rayleigh flat fading channel.

Keywords
Filter Bank Multicarrier (FBMC), offset QAM (OQAM), μ-law companding, A-law companding, rooting companding, tangent rooting companding, logarithmic rooting companding, turbo codes, low-density parity check (LDPC) codes

1. INTRODUCTION
Filter Bank Multicarrier (FBMC) is a potential multicarrier waveform contender for 5G and future wireless standards because of its various advantages such as lowest out-of-band leakage among various multicarrier waveform candidates, high spectral efficiency, and ability to work in asynchronous scenarios [1], [2]. Being a multicarrier waveform technique, it suffers from high peak-to-average-power ratio (PAPR) problem. For waveforms with high PAPR a high-power amplifier is forced to operate at reduced power efficiency [3], [4]. Companding techniques as compared to other PAPR reduction techniques such as Selective Mapping (SLM), and Partial Transmit Sequence (PTS) have lower computational complexity and no effective data rate reduction. Companding expands the small signal values and compresses the large signal values. Non-linear companding techniques cause bit-error-rate (BER) degradation in systems because inverse companding performed at the receiver magnifies the channel noise. This magnified channel noise is called the companding noise [5].

In [6], clipping, A-law and μ-law non-linear companding techniques are examined for PAPR reduction of FBMC/offset QAM (OQAM)signals. In [7], Hadamard transform is combined with exponential companding to reduce PAPR of FBMC signals. In [8], tone injection is combined with μ-law companding to lower PAPR of FBMC/OQAM signals. In [9], A-law and μ-law companding transforms are analyzed by varying the values of companding parameters for PAPR reduction of FBMC/OQAM system. In [10] A-law companding, μ-law companding, clipping and filtering techniques are examined for PAPR reduction of FBMC signals using various modulation schemes. In [11], A-law, μ-law, hyperbolic tangent, error function, and logarithmic non-linear companding techniques, are investigated to lower PAPR of FBMC/OQAM signals. In [12], Discrete Sine Transform (DST) precoding combined with A-law companding is used to reduce PAPR of FBMC/OQAM signals. In [13], authors have proposed a modified square rooting companding technique to reduce PAPR of FBMC/OQAM signals. In [14], absolute exponential companding scheme is utilized for PAPR reduction of FBMC/OQAM signals. In [15], a hybrid scheme using trellis-based selective mapping (TSLM) combined with A-Law companding is proposed to lower PAPR of FBMC/OQAM signals. In [16], μ-law, A-law, rooting, tangent rooting, logarithmic rooting and absolute exponential non-linear companding techniques are analyzed theoretically and by experimentation in terms of PAPR reduction for FBMC/OQAM signals. In [17], μ-law, A-law, rooting, tangent rooting, and logarithmic rooting companding techniques are investigated in terms of PAPR reduction performance and BER performance for FBMC/OQAM signals in additive white Gaussian noise (AWGN) channel.

Channel coding also known as forward error correction improves the reliability of a system but at the expense of increased system complexity and additional bandwidth requirement. In [18] turbo coded Orthogonal Frequency Division Multiplexing (OFDM) and FBMC systems are analyzed in the presence of phase noise. In [19], authors have proposed a turbo coded MIMO-FBMC system and compared it with a turbo coded MIMO-OFDM system. In [20], turbo coded and uncoded massive MIMO-FBMC system is compared with turbo coded and uncoded massive MIMO-

OFDM system in underwater acoustic channel in terms of BER performance for real-time video transmission. In [21], a parallel coding scheme using turbo product code is proposed for mobile multimedia data transmission over a MIMO-FBMC system. In [22], low-density parity check (LDPC) coded FBMC system is analyzed. In [23], LDPC coded FBMC system is proposed for data transmission over underwater acoustic channel. In [24], application of non-binary LDPC codes to FBMC/OQAM system is investigated. In [25], LDPC coded MIMO-FBMC system is proposed for transmission of multimedia signals over underwater acoustic channel. In [26], LDPC coded FBMC system is proposed for voice and image transmission over underwater acoustic channel.

FBMC can be implemented either using polyphase network (PPN)-FFT or Frequency Spread (FS)-FBMC implementation [27]. In this work FS-FBMC implementation is used.

In [17], it was shown that logarithmic rooting companding provides maximum PAPR reduction gain (among the various companding techniques) as compared to a conventional FS-FBMC/OQAM system without companding. Also, in [17] BER analysis of the various companding techniques for FS-FBMC/OQAM signals was performed in AWGN channel. It was observed that the μ-law companding provided better BER performance in comparison to other companding schemes in AWGN channel. In this paper, μ-law, A-law, rooting, tangent rooting, and logarithmic rooting companding transforms were investigated and compared in terms of BER performance for FS-FBMC/OQAM signals in both slow and fast Rayleigh flat fading channels. It was observed that the rooting companding provided better BER performance in comparison to other companding schemes in both slow and fast Rayleigh flat fading channels.

Also, turbo coded and LDPC coded FS-FBMC/OQAM systems were investigated and compared in terms of their PAPR values and BER performance over both slow and fast Rayleigh flat fading channels, which was not explored in any of the earlier works. It was observed that LDPC coded and turbo coded FS-FBMC/OQAM system provided almost similar amount of coding gain in comparison to an uncoded FS-FBMC/OQAM system, but LDPC coded FS-FBMC/OQAM system provided slightly better BER performance as compared to turbo coded FS-FBMC/OQAM system. Also, LDPC coded FS-FBMC/OQAM system provided lower PAPR value in comparison to turbo coded FS-FBMC/OQAM system. Also, in the Rayleigh flat fading channel, the FS-FBMC/OQAM system outperforms the OFDM system in terms of BER performance.

This paper is organized as follows: in Section 2, FS-FBMC/OQAM system is discussed. In Section 3, different non-linear companding techniques for PAPR reduction of FS-FBMC/OQAM signals are presented. In Section 4, turbo codes and LDPC codes are discussed. Section 5 presents the proposed coded FS-FBMC/OQAM system. In Section 6, the simulation results are presented and the discussions on the results obtained are stated. Finally, in Section 7 paper is concluded based on the results obtained.

2. FS-FBMC/OQAM SYSTEM

FBMC is a multicarrier waveform technique in which all the subcarriers are filtered individually using non-rectangular pulse shaping filters. The FBMC symbol extends over K symbol intervals and overlaps with K successive FBMC symbols. K is called the overlapping factor. Figure 1 [17] depicts the FS-FBMC/OQAM transceiver block diagram. PPN-FFT FBMC receiver requires time domain subcarrier multi tap equalization to be performed that causes further transmission delay. FS-FBMC receiver requires one tap frequency domain equalization for each subcarrier that creates no further delay. FS-FBMC transceiver needs extended IFFT and FFT of sizes KN. Here, N is the total number of subcarriers. PPN-FFT transceiver needs IFFT and FFT of sizes N, and KN extra multiplications for the PPN [27].

The frequency spreading [28] operation can be explained using the following equation:

$$S_{lK+k} = F_k \times d_l \quad (1)$$

where, $S(p')$ with index$lK + k$ are the subcarriers at the input of extended IFFT, $d(p)$with index l,are the inputs of frequency spreading and filtering block such that $d(p)$ is a sequence of real and imaginary parts (imaginary parts are multiplied by imaginary term 'j') of complex modulated symbols that alternate to ensure real field orthogonality among subcarriers $S(p')$, and F_k are the frequency domain coefficients of prototype filter such that $F_k = F_{-k}$.

Here, p=0 to N-1, l=1 to N, p′= 0 to KN-1, and k= -(K-1) to (K-1)

Output of the extended IFFT block $s(n')$can be stated using the following equation:

$$s(n') = \frac{1}{\sqrt{KN}} \sum_{p'=0}^{KN-1} S(p') e^{j2\pi p' n'/KN} \quad (2)$$

where, n′=0 to KN-1

OQAM is used to double the symbol rate and achieve full capacity. Successive extended IFFT outputs are generated by interchanging the mapping of the real part and the imaginary part of complex modulated symbols at the inputs of the frequency spreading and filtering block. Successive extended IFFT outputs of duration KN are overlapped with a delay of N/2, then summated up and transmitted over a channel. The output of the FS-FBMC/OQAM transmitter in time domain is stated as:

$$x_{FBMC}(n) = \sum_{g=0}^{T_0-1} s_g(n - gN/2) \quad (3)$$

where, $n = 0\ to\ (K + T_0/2)\ N - N/2 - 1$

where, T_0 is the total number of FS-FBMC/OQAM symbols, and $s_g(n')$ is the gth extended IFFT output.

The received FS-FBMC/OQAM signal $r_{FBMC}(n)$ is expressed as:

$$r_{FBMC}(n) = x_{FBMC}(n) + w(n) \quad (4)$$

Where w(n) is the channel noise signal.

The receiver considers $r_{FBMC}(n)|_{\text{ n= 0 to KN-1}}$ as the first FS-FBMC/OQAM symbol, $r_{FBMC}(n)|_{\text{ n= KN to 2KN-1}}$ as the second FS-FBMC/OQAM symbol and so on.

The frequency de-spreading [28] operation performed at the receiver side can be explained using the following equation:

$$d_l^{'} = \sum_{k=-(K-1)}^{K-1} S'_{lK+k} \times F_k \quad (5)$$

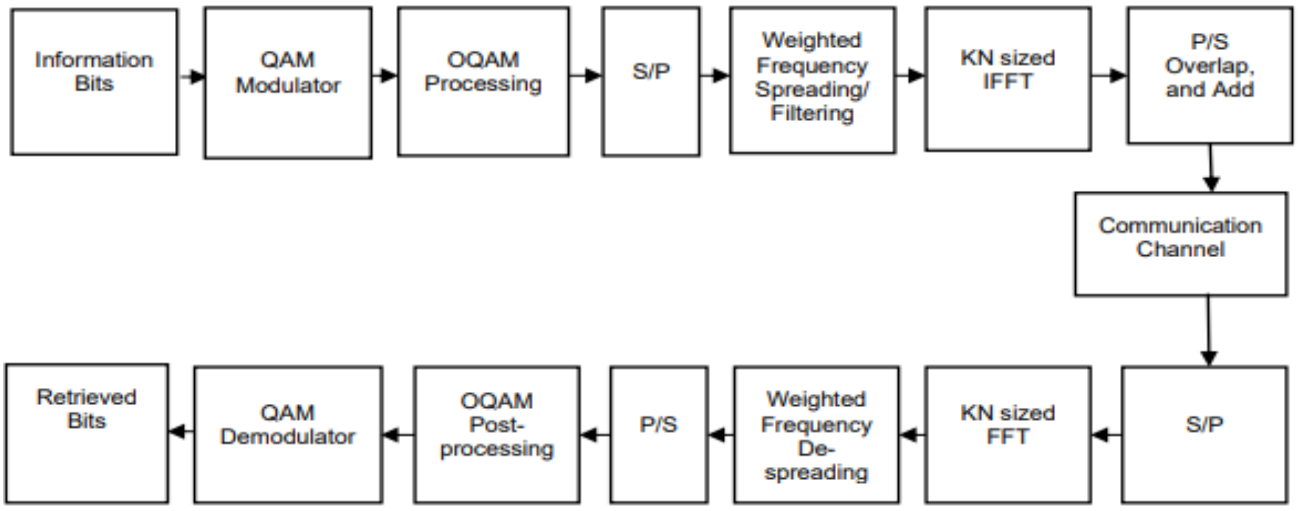

Fig 1: FS-FBMC/OQAM system block diagram

where, $d^{'}(p)$ indexed as, l,are the outputs of the frequency de-spreading and filtering block, and $S'(p')$ with index $lK + k$ are the inputs of the frequency de-spreading and filtering block.

3. PEAK-TO-AVERAGE POWER RATIO (PAPR) REDUCTION TECHNIQUES

PAPR of FS-FBMC/OQAM signal x[n]can be stated as:

$$PAPR(dB) = 10\,log_{10}\left(\frac{max_{\,0\le n\le KN-1}|x[n]|^2}{E[|x[n]|^2]}\right) \quad (6)$$

where, $x(n) = x_{FBMC}(n)|_{n=0\ to\ KN-1}$

The complementary cumulative distribution function (CCDF) of PAPR values measures the PAPR reduction capability of a scheme. It can be expressed as the function of a threshold value, $PAPR_0$ as probability, P, that PAPR is greater than $PAPR_0$, and is expressed as:

$$CCDF(PAPR_0) = P(PAPR > PAPR_0) \quad (7)$$

The different non-linear companding techniques used to lower the PAPR of FS-FBMC/OQAM signal x[n]are given below:

3.1 μ-law companding

The μ-law companded [6, 9, 11, 16, 17] FS-FBMC/OQAM signal can be stated using the following equation:

$$C(x[n]) = \frac{log_e(1+\mu|x[n]|)}{log_e(1+\mu)}\ sgn(x[n]) \quad (8)$$

where C is the companding function, μ is the companding parameter that determines the degree of companding, and sgn is the signum function.

The μ-law inverse companded signal can be stated using the following equation:

$$C^{-1}(r[n]) = \frac{sgn(r[n])}{\mu}\ ((1+\mu)^{|r[n]|} - 1) \quad (9)$$

Here, C^{-1} is the inverse companding function, r[n] is the received companded FS-FBMC/OQAM signal over a communication channel.

3.2 A-law companding

The A-law companded [6, 9, 11, 16, 17] FBMC signal can be stated using the following equation:

$$C(x[n]) = sgn(x[n])\frac{A|x[n]|}{(1+log_eA)}, \quad when\ |x[n]| < 1/A$$

$$C(x[n]) = sgn(x[n])\ \frac{(1+log_e(A|x[n]|))}{(1+logA)},$$
$$when\ \frac{1}{A} \le |x[n]| < 1 \quad (10)$$

where A is the companding parameter that decides the degree of companding.

The A-law inverse companded signal can be stated using the following equation:

$$C^{-1}(r[n]) = sgn(r[n])\frac{|r[n]|(1+log_eA)}{A},$$
$$when\ |r[n]| < 1/(1+log_eA)$$
$$C^{-1}(r[n]) = sgn(r[n])\frac{\exp(|r[n]|(1+log_eA)-1)}{A},$$
$$when\ 1/(1+log_eA) \le |r[n]| < 1 \quad (11)$$

3.3 Rooting companding

The rooting companded [13, 16, 17] FS-FBMC/OQAM signal can be stated using the following equation:

$$C(x[n]) = |x[n]|^R sgn(x[n]) \quad (12)$$

where R is the companding parameter varying from 0.1 to 0.9.

The rooting inverse companded signal can be stated using the following equation:

$$C^{-1}(r[n]) = |r[n]|^{1/R} sgn(r[n]) \quad (13)$$

3.4 Tangent Rooting companding

The tangent rooting companded [16, 17] FS-FBMC/OQAM signal can be stated using the following equation:

$$C(x[n]) = \tanh(|x[n]| \times L)^R)\ sgn(x[n]) \quad (14)$$

where L is the companding parameter varying from 5 to 25, and it decides the degree of companding, and R is the companding parameter varying from 0.1 to 1.

The tangent rooting inverse companded signal can be stated using the following equation:

$$C^{-1}(r[n]) = \left|\left(\text{atanh}\left(\frac{|r[n]|}{L}\right)\right)^{\frac{1}{R}}\right| sgn(r[n]) \quad (15)$$

3.5 Logarithmic Rooting companding

The logarithmic rooting companded [16, 17] FS-FBMC/OQAM signal can be stated using the following equation:

$$C(x[n]) = log_e((|x[n]| \times L)^R + 1)\, sgn(x[n]) \qquad (16)$$

where L is the companding parameter that decides the degree of companding, and R is the companding parameter limiting the PAPR reduction ability of the companding technique.

The logarithmic rooting inverse companded signal can be stated using the following equation:

$$C^{-1}(r[n]) = \left|\left(\exp\left(\frac{|r[n]|}{L}\right) - 1\right)^{\frac{1}{R}}\right| sgn(r[n]) \qquad (17)$$

4. CHANNEL CODES

4.1 Turbo codes

A turbo encoder is a recursive systematic encoder with two recursive systematic convolutional encoders connected in parallel [29]. The input bit sequence is passed through the second convolutional encoder after the application of a certain pseudorandom interleaving algorithm.

The turbo decoding uses either of the following two algorithms: Log-Maximum A Posteriori (MAP) or Max-Log-MAP for a given number of iterations [29].

Here an iterative Max-Log-MAP turbo decoding algorithm is used which is a simplified version of Log-MAP.

Turbo codes with large interleavers come with certain disadvantages such as increased decoding delay and the iterative decoding algorithm of high computational complexity. However, most communication systems for the sake of achieving significantly high coding gain endure the decoding delay, and the increased computational complexity [29].

Turbo codes are used in several wireless systems such as WCDMA, LTE, DVB, and WiMAX [30], [31].

4.2 LDPC codes

Low-Density Parity Check (LDPC) code is a type of linear error-correction code having a parity check matrix H, that is sparse (a smaller number of nonzero elements in each column and row of matrix, H) [32]. LDPC codes can be represented in two ways: one using parity check matrix, H and other using graphical representation i.e., using bipartite graph [33].

Consider code word length is represented by n_0, and the no. of information bits is represented by k_0, and m_0 represents the no. of parity bits, then code rate, $R_c = k_0/n_0$. Consider u represents uncoded input bits then, codeword c is represented as [33]:

$$c = uG \qquad (18)$$

where,

$$G_{k_0 \times n_0} = [I_{k_0} P_{k_0 \times (n_0 - k_0)}] \qquad (19)$$

G is the generator matrix of dimension $k_0 \times n_0$, I_{k_0} is the identity matrix of dimension $k_0 \times k_0$ and P is parity matrix of dimension $k_0 \times (n_0 - k_0)$. Parity Check Matrix, H is expressed as [33]:

$$H_{(n_0 - k_0) \times n_0} = [P^T I_{n_0 - k_0}] \qquad (20)$$

Due to the orthogonality between matrices G and H [33]:

$$HG^T = 0 \qquad (21)$$

LDPC decoder uses either soft decision decoding algorithms or hard decision decoding. Soft decision decoding algorithms provide significantly good BER performance but at the cost of increased computational complexity and decoding delay. Hard decision decoding algorithms provide lower decoding delay at the cost of reduced BER performance [33].

In this work soft decision hard output iterative Belief Propagation decoding algorithm having low computational complexity and low decoding delay [33] is used.

LDPC codes are used in several wireless systems and standards such as DVB-S2, WiMAX 802.16e, Wireless LAN 802.11n, Wireless RAN 802.22 [32, 33]. Also, LDPC codes are contenders for 5G channel codes [33].

Figure 2 shows the BER performance of turbo and LDPC codes using 4-QAM in Rayleigh flat fading channel with doppler spread, f_s=5 Hz for code rate, R_c=1/3. Figure 3 shows the BER performance of turbo and LDPC codes using 4-QAM in Rayleigh flat fading channel with f_s=80 Hz for code rate, R_c=1/3.

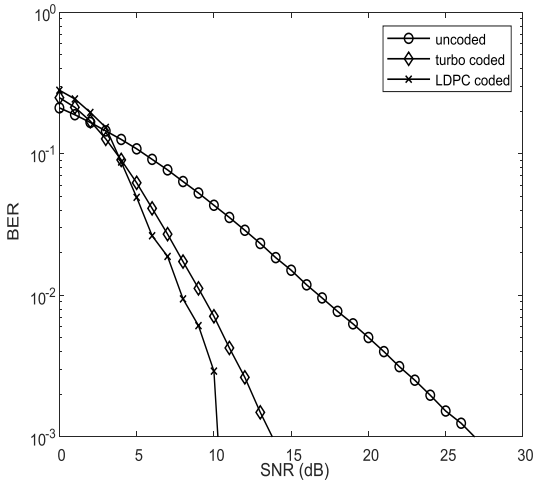

Fig 2: BER performance of turbo and LDPC codes using 4-QAM in Rayleigh flat fading channel with f_s=5 Hz for code rate, R_c=1/3

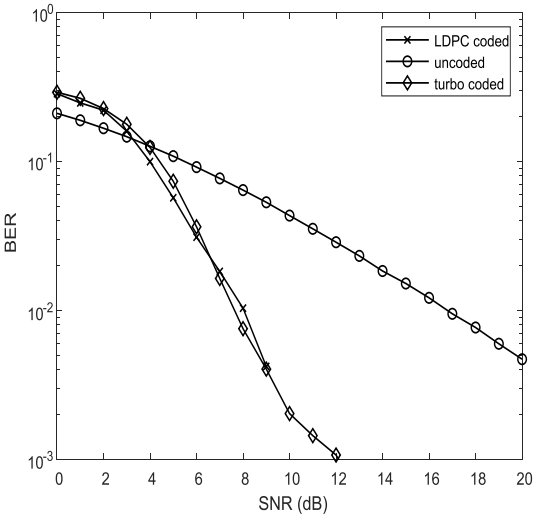

Fig 3: BER performance of turbo and LDPC codes using 4-QAM in Rayleigh flat fading channel with f_s=80 Hz for code rate, R_c=1/3

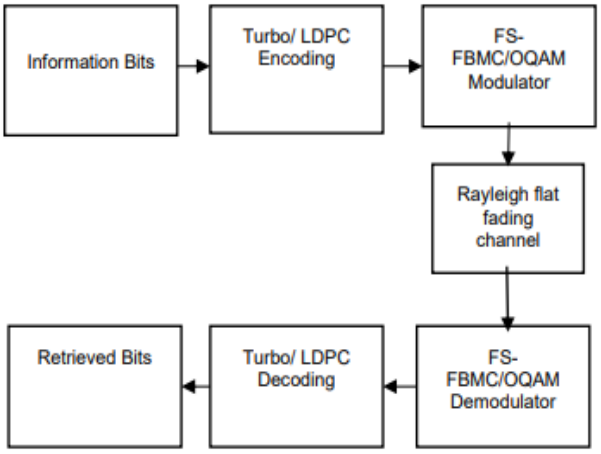

Fig 4: Proposed coded FS-FBMC/OQAM system

5. PROPOSED CODED FS-FBMC/OQAM SYSTEM

Figure 4 shows the block diagram of the proposed coded FS-FBMC/OQAM system coded using either turbo codes or LDPC codes. The randomly generated data bits are passed through a turbo encoder or a LDPC encoder, then modulated using FS-FBMC/OQAM modulator as discussed in Section 2. Then the coded FS-FBMC/OQAM signal is passed through a Rayleigh flat fading channel. At the receiver received FS-FBMC/OQAM symbols are first demodulated using FS-FBMC/OQAM demodulator as discussed in Section 2, then finally the data bits are decoded using either turbo decoder or LDPC decoder. Perfect channel estimation is assumed at the receiver side.

For turbo and LDPC codes, the total number of operations (Additions, Multiplications, Complex operations) per code word can be stated using (22) and (23) accordingly [34]:

$$T_{turbo} \cong 5 \times 10^4 L \qquad (22)$$

where, T_{turbo} is the total number of operations per code word for turbo codes, and L is the length of the codeword.

$$T_{LDPC} \cong 0.8 \times 10^4 L \qquad (23)$$

where, T_{LDPC} is the total number of operations per code word for LDPC codes. Hence, LDPC decoding requires fewer operations per code word length than turbo decoding:

$$T_{turbo} \cong 6\, T_{LDPC} \qquad (24)$$

6. RESULTS AND DISCUSSION

The FS-FBMC/OQAM system companded using techniques mentioned in Section 3 was analyzed in terms of BER performance in Rayleigh flat fading channels. Two channel types were considered: slow fading with doppler spread =fs=5 Hz and fast fading with doppler spread =fs=80 Hz. The number of subcarriers was set to N=1024 (Guard band given 424 subcarriers).Overlapping factor was set to K=4. Frequency domain coefficients of the prototype filter, F_k were used as given in the PHYDYAS project [28]. 4-QAM modulation was used. Companding parameters were set to μ=5, A=5, R=0.4, and L=5. Simulations were performed in MATLAB.

Figure 5 shows the BER performance of various companding techniques for different values of signal-to-noise ratio (SNR) for FS-FBMC/OQAM systems in Rayleigh flat fading channel with fs=5 Hz. Figure 6 shows the BER performance of various companding techniques for different values of SNR for FS-FBMC/OQAM systems in Rayleigh flat fading channel with fs=80 Hz. It can be observed that rooting companding provides better BER performance as compared to other companding techniques in Rayleigh flat fading channels. Companding causes BER performance degradation of FS-FBMC/OQAM system because of the introduction of companding noise. It can be observed that by increasing the value of parameter, R from 0.4 to 0.5, the BER performance of rooting and logarithmic rooting companding improves but at the cost of reduced PAPR reduction performance as shown in [13, 17].

The proposed coded FS-FBMC/OQAM system was analyzed in terms of BER performance in Rayleigh flat fading channels and in terms of PAPR. The number of coded subcarriers was set to N=65224 and the number of uncoded subcarriers was set to N′=22024 for both FS-FBMC/OQAM and OFDM systems. 4-QAM modulation was used. Soft decision hard output Max-Log-MAP decoding algorithm was used for turbo decoding with 4 iterations. Soft decision hard output Belief Propagation decoding algorithm was used for LDPC decoding with maximum number of iterations set to 50. Simulations were performed in MATLAB using the parameter values given in Table 1.

Table 1. Parameter values of LDPC codes and turbo codes

	Parameters	**Values**
LDPC code	Code rate, R_c	1/3
	Parity check matrix, H	As used in DVB-S2 standard
Turbo code	Code rate, R_c	1/3
	Constraint length	4
	Generator matrix	$[13\ 15]_{octal}$

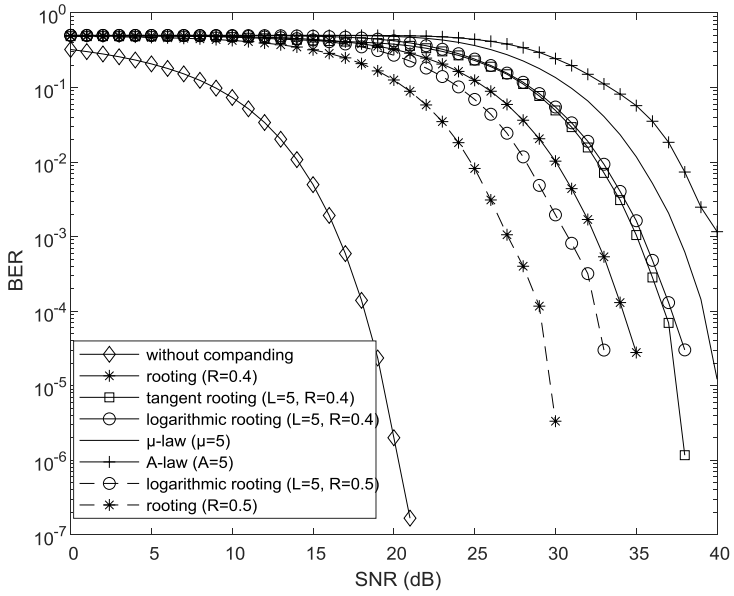

Fig 5:BER performance of various companding techniques for FS-FBMC/OQAM systems in Rayleigh flat fading channel with f_s=5 Hz

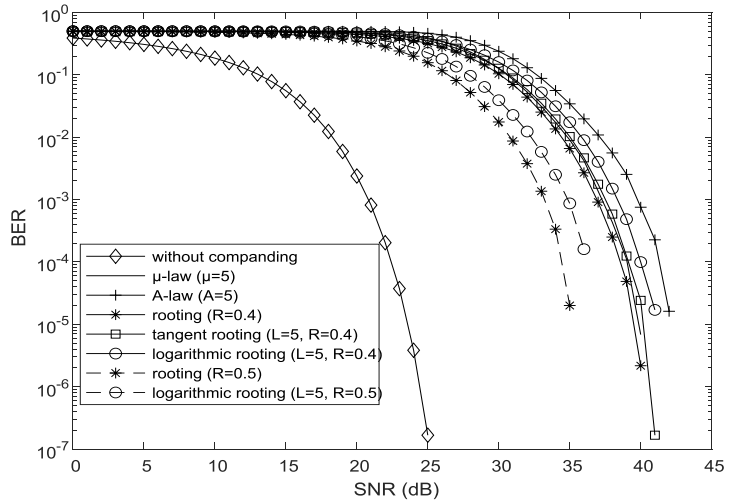

Fig 6: BER performance of various companding techniques for FS-FBMC/OQAM systems in Rayleigh flat fading channel with f_s=80 Hz

Figure 7 shows the BER performance of turbo and LDPC coding techniques for different values of SNR for FS-FBMC/OQAM systems in Rayleigh flat fading channel with fs=5 Hz. Figure 8 shows the BER performance of turbo and LDPC coding techniques for different values of SNR for FS-FBMC/OQAM systems in Rayleigh flat fading channel with fs=80 Hz. It can be observed that both turbo codes and LDPC codes provide a coding gain of about 7 dB at BER=10^{-2} as compared to uncoded FS-FBMC/OQAM system in Rayleigh flat fading channel with fs=5 Hz. It can be observed that turbo codes and LDPC codes both provide a coding gain of about 4 dB at BER=10^{-2} as compared to uncoded FS-FBMC/OQAM system in Rayleigh flat fading channel with fs=80 Hz. It can be observed that LDPC coded FS-FBMC/OQAM system provides slightly better BER performance as compared to turbo coded FS-FBMC/OQAM system because LDPC coded FS-FBMC/OQAM system provides BER=0 at SNR= 9 dB and turbo coded FS-FBMC/OQAM system provides BER=0at SNR=10 dB in Rayleigh flat fading channel with fs=5 Hz. Also, LDPC coded FS-FBMC/OQAM system providesBER=0 at SNR=12 dB and turbo coded FS-FBMC/OQAM system provides BER=0 at SNR=13 dB in Rayleigh flat fading channel with fs=80 Hz.

Table 2 shows the PAPR values obtained using turbo coded, LDPC coded and uncoded FS-FBMC/OQAM systems. It can be observed that LDPC coded FS-FBMC/OQAM system provides a lower PAPR value as compared to turbo coded FS-FBMC/OQAM. Also, incorporation of channel coding slightly increases the PAPR of the system (by about 1 to 1.6 dB) in addition to the high coding gain(about 4 to 7 dB at BER=10^{-2}) achieved as shown in Figure 7 and Figure 8, because the number of subcarriers is increased from 22024 to 65224.

Hence, it can be concluded that LDPC coded FS-FBMC/OQAM due to its better BER and PAPR performances can be chosen for applications requiring reduced computational complexity and decoding delay. As, LDPC decoder requires lesser number of operations per a given code word length as compared to turbo decoder (shown in equation 24).

Figure 9 shows the BER performance comparison of FS-FBMC/OQAM and OFDM systems for different values of SNR in Rayleigh flat fading channel with fs=5 Hz. It can be observed that coded FS-FBMC/OQAM systems outperform coded OFDM systems. Also, uncoded FS-FBMC/OQAM system outperforms uncoded OFDM system.

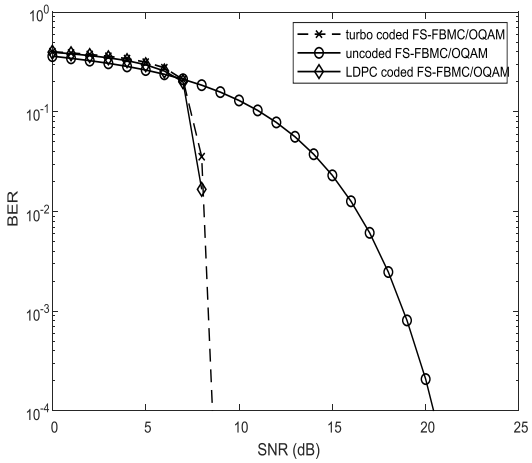

Fig 7:BER performance of turbo and LDPC coding techniques for FS-FBMC/OQAM systems in Rayleigh flat fading channel with fs=5 Hz

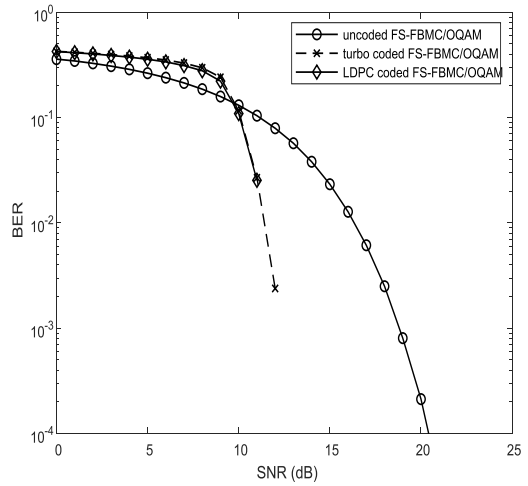

Fig 8:BER performance of turbo and LDPC coding techniques for FS-FBMC/OQAM systems in Rayleigh flat fading channel with fs=80 Hz

Table 2. PAPR values obtained using coded and uncoded FS-FBMC/OQAM systems

Proposed system	PAPR (dB) at CCDF=10^{-4}
Turbo coded FS-FBMC/OQAM system	13.46
LDPC coded FS-FBMC/OQAM system	12.83
Uncoded FS-FBMC/OQAM system	11.84

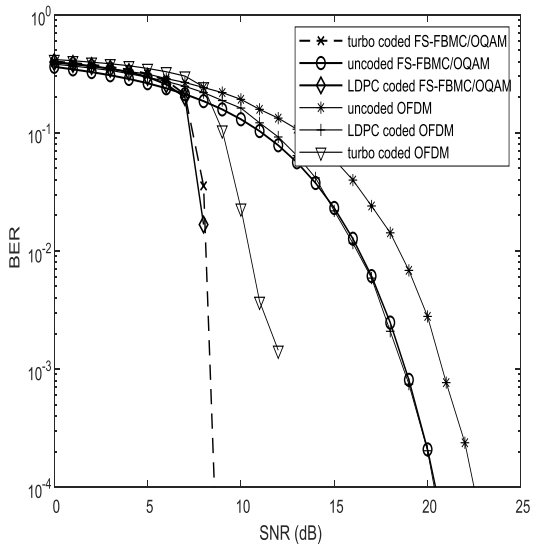

Fig 9: BER performance comparison of FS-FBMC/OQAM and OFDM systems in Rayleigh flat fading channel

7. CONCLUSIONS

In this paper PAPR and BER analysis of various companding techniques was performed for FS-FBMC/OQAM system in Rayleigh flat fading channels. It was observed that rooting companding provided better BER performance as compared to other companding techniques in Rayleigh flat fading channels. It was also observed that LDPC coded FS-FBMC/OQAM system provided slightly better BER performance as compared to turbo coded FS-FBMC/OQAM system in Rayleigh flat fading channels. Also, LDPC coded FS-FBMC/OQAM system provided lower PAPR value as compared to turbo coded FS-FBMC/OQAM and is suitable for applications requiring lower computational complexity and delay. It was also observed that FS-FBMC/OQAM system outperforms OFDM system in terms of BER performance in Rayleigh flat fading channel.

8. REFERENCES

[1] Maziar, N., Yue, W., Milos, T., Shangbin, W., Yinan, Q., & Mohammed, A. I. (2016). Overview of 5G modulation and waveforms candidates. Journal of communications and Information Networks, 1(1), 44-60.

[2] Cai, Y., Qin, Z., Cui, F., Li, G. Y., & McCann, J. A. (2017). Modulation and multiple access for 5G networks. IEEE Communications Surveys & Tutorials, 20(1), 629-646.

[3] Zhao, J., Ni, S., & Gong, Y. (2017). Peak-to-average power ratio reduction of FBMC/OQAM signal using a joint optimization scheme. IEEE Access, 5, 15810-15819.

[4] Wang, H., Wang, X., Xu, L., & Du, W. (2016). Hybrid PAPR reduction scheme for FBMC/OQAM systems based on multi data block PTS and TR methods. IEEE Access, 4, 4761-4768.

[5] Jiang, T., & Wu, Y. (2008). An overview: Peak-to-average power ratio reduction techniques for OFDM signals. IEEE Transactions on broadcasting, 54(2), 257-268.

[6] Varghese, N., Chunkath, J., &Sheeba, V. S. (2014,

August). Peak-to-average power ratio reduction in FBMC-OQAM system. In 2014 Fourth International Conference on Advances in Computing and Communications (pp. 286-290). IEEE.

[7] Elmaroud, B., Faqihi, A., Abbad, M., &Aboutajdine, D. (2014, June). PAPR reduction of FBMC signals by combining exponential companding and Hadamard transforms. In The 2014 International Symposium on Networks, Computers and Communications (pp. 1-4). IEEE.

[8] Gopal, R., & Patra, S. K. (2015, April). Combining tone injection and companding techniques for PAPR reduction of FBMC-OQAM system. In 2015 Global Conference on Communication Technologies (GCCT) (pp. 709-713). IEEE.

[9] Hasan, A., Zeeshan, M., Mumtaz, M. A., & Khan, M. W. (2018, May). PAPR reduction of FBMC-OQAM using A-law and Mu-law companding. In 2018 ELEKTRO (pp. 1-4). IEEE.

[10] Kumar, A., & Rathore, H. (2018). Reduction of PAPR in FBMC system using different reduction techniques. Journal of Optical Communications.

[11] Shaheen, I. A., Zekry, A., Newagy, F., & Ibrahim, R. (2019). Performance evaluation of PAPR reduction in FBMC system using nonlinear companding transform. ICT Express, 5(1), 41-46.

[12] Shaheen, I. A., Zekry, A., Newagy, F., & Ibrahim, R. (2017, October). PAPR reduction of FBMC/OQAM systems based on combination of DST precoding and A-law nonlinear companding technique. In 2017 International Conference on Promising Electronic Technologies (ICPET) (pp. 38-42). IEEE.

[13] Shaheen, I. A., Zekry, A., Newagy, F., & Ibrahim, R. (2017, May). Modified square rooting companding technique to reduced PAPR for FBMC/OQAM. In 2017 Palestinian international conference on information and communication technology (PICICT) (pp. 66-70). IEEE.

[14] Shaheen, I. A. A., Zekry, A., Newagy, F., & Ibrahim, R. (2017, May). Absolute Exponential Companding to Reduced PAPR for FBMC/OQAM. In 2017 Palestinian International Conference on Information and Communication Technology (PICICT) (pp. 60-65). IEEE.

[15] Li, X., Wang, D., Li, Z., Bai, W., Hu, X., & Fu, R. (2020, June). A Hybrid TSLM and A-Law Companding Scheme for PAPR Reduction in FBMC-OQAM Systems. In 2020 International Wireless Communications and Mobile Computing (IWCMC) (pp. 1077-1081). IEEE.

[16] Ramavath, S., &Samal, U. C. (2021). Theoretical Analysis of PAPR Companding Techniques for FBMC Systems. Wireless Personal Communications, 118(4), 2965-2981.

[17] Mobin, A., & Ahmad, A. (2021, September). PAPR reduction of FBMC-OQAM systems using logarithmic rooting companding. In 2021 Fourth International Conference on Electrical, Computer and Communication Technologies (ICECCT) (pp. 1-6). IEEE.

[18] Roth, K., Baltar, L. G., Faerber, M., &Nossek, J. A. (2017, June). Performance analysis of FBMC and CP-OFDM in the presence of phase noise. In 2017 European Conference on Networks and Communications (EuCNC) (pp. 1-5). IEEE.

[19] Mathews, L., & Pillai, S. S. (2016, December). Performance of turbo coded FBMC based MIMO systems. In 2016 IEEE International Conference on Computational Intelligence and Computing Research (ICCIC) (pp. 1-5). IEEE.

[20] Bocus, M. J., Agrafiotis, D., &Doufexi, A. (2018, April). Real-time video transmission using massive MIMO in an underwater acoustic channel. In 2018 IEEE wireless communications and networking conference (WCNC) (pp. 1-6). IEEE.

[21] Li, Z., Miao, M., & Wang, Z. (2019). Parallel Coding Scheme With Turbo Product Code for Mobile Multimedia Transmission in MIMO-FBMC System. IEEE Access, 8, 3772-3780.

[22] Jo, S., &Seo, J. S. (2015). Tx scenario analysis of FBMC based LDM system. ICT Express, 1(3), 138-142.

[23] Lin, C. F., Su, T. J., Chang, S. H., Parinov, I. A., &Shevtsov, S. N. (2020). Direct Mapping Based FBMC-LDPC Advanced Underwater Acoustic Transmission Scheme for Data Signals. In Advanced Materials (pp. 597-603). Springer, Cham.

[24] Caus, M., Navarro, M., Mestre, X., & Pérez-Neira, A. (2016, June). Link adaptation in FBMC/OQAM systems using NB-LDPC codes. In 2016 European Conference on Networks and Communications (EuCNC) (pp. 11-15). IEEE.

[25] Lin, C. F., Su, T. J., Chang, H. K., Lee, C. K., Chang, S. H., Parinov, I. A., &Shevtsov, S. (2020). Direct-Mapping-Based MIMO-FBMC underwater acoustic communication architecture for multimedia signals. Applied Sciences, 10(1), 233.

[26] Lin, C. F., Hung, Y. T., Lu, H. W., Chang, S. H., Parinov, I. A., &Shevtsov, S. (2018). FBMC/LDPC-based underwater transceiver architecture for voice and image transmission. Journal of Marine Science and Technology, 26(3), 4.

[27] Bellanger, M. (2012, December). FS-FBMC: A flexible robust scheme for efficient multicarrier broadband wireless access. In 2012 IEEE Globecom Workshops (pp. 192-196). IEEE.

[28] Bellanger, M., Le Ruyet, D., Roviras, D., Terré, M., Nossek, J., Baltar, L., ... &Ihalainen, T. (2010). FBMC physical layer: a primer. Phydyas, 25(4), 7-10.

[29] Proakis, J. G., & Salehi, M. (2008). Digital communications 5th Edition McGraw-Hill. New York.

[30] Berrou, C., Pyndiah, R., Adde, P., Douillard, C., & Le Bidan, R. (2005, October). An overview of turbo codes and their applications. In The European Conference on Wireless Technology, 2005. (pp. 1-9). IEEE.

[31] Long, X., Chen, Q., Xiao, P., & Wu, J. (2012, December). On the design of PS-RCPT codes for LTE system. In 2012 IEEE global communications conference (GLOBECOM) (pp. 4238-4243). IEEE.

[32] Hajiyat, Z. R. M., Sali, A., Mokhtar, M., & Hashim, F. (2019). Channel coding scheme for 5G mobile communication system for short length message transmission. Wireless Personal Communications,

106(2), 377-400.

[33] Arora, K., Singh, J., & Randhawa, Y. S. (2019). A survey on channel coding techniques for 5G wireless networks. Telecommunication Systems, 1-27.

[34] Fagervik, K., &Larssen, A. S. (2003, October). Performance and complexity comparison of low density parity check codes and turbo codes. In Proc. Norwegian Signal Processing Symposium, (NORSIG'03) (pp. 2-4).